Immature Midbrain Dopaminergic Neurons Derived from Floor-Plate Method Improve Cell Transplantation Therapy Efficacy for Parkinson's Disease

LIFENG QIU (ORCID),[a*] MEI-CHIH LIAO,[b*] ALLEN K. CHEN,[b] SHUNHUI WEI,[c] SHAOPING XIE,[d] SHAUL REUVENY,[b] ZHI DONG ZHOU,[d,e] WALTER HUNZIKER,[c,f] ENG KING TAN,[d,e,g] STEVE K. W. OH,[b] LI ZENG[a,e]

Key Words. Midbrain dopaminergic neurons • Floor-plate • Transplantation • Parkinson's disease • Differentiation • Tyrosine hydroxylase

[a]Neural Stem Cell Research Lab, Research Department, National Neuroscience Institute, Singapore; [b]Stem Cell Group, Bioprocessing Technology Institute, Agency for Science, Technology and Research, Singapore; [c]Epithelial Cell Biology Laboratory, Institute of Molecular and Cell Biology, Singapore; [d]Research Department, National Neuroscience Institute, Singapore; [e]Neuroscience & Behavioral Disorders Program, DUKE-NUS Graduate Medical School, Singapore; [f]Department of Physiology, National University of Singapore, Singapore; [g]Department of Neurology, National Neuroscience Institute, Singapore

Correspondence: Eng King Tan, M.D., Research Department, National Neuroscience Institute, Singapore 308433. Telephone: +65 6326 5003; Fax: +65 6220 3321; e-mail: tan.eng.king@sgh.com.sg; or Steve Oh, Ph.D., Stem Cell Group, Bioprocessing Technology Institute, Agency for Science, Technology and Research, Singapore 138668. Telephone: +65 6407 0855, Fax: +65 6478 9561; e-mail: Steve_Oh@bti.a-star.edu.sg. Li Zeng, Ph.D., Neural Stem Cell Research Lab, Research Department, National Neuroscience Institute, Singapore 308433. Telephone: +65 6357 7515; Fax: +65 6256 9178; e-mail: Li_Zeng@nni.com.sg

*Contributed equally.

ABSTRACT

Recent reports have indicated human embryonic stem cells-derived midbrain dopamine (mDA) neurons as proper cell resources for use in Parkinson's disease (PD) therapy. Nevertheless, no detailed and systematic study has been conducted to identify which differentiation stages of mDA cells are most suitable for transplantation in PD therapy. Here, we transplanted three types of mDA cells, DA progenitors (differentiated in vitro for 16 days [D16]), immature DA neurons (D25), and DA neurons (D35), into PD mice and found that all three types of cells showed high viability and strong neuronal differentiation in vivo. Both D25 and D35 cells showed neuronal maturation and differentiation toward TH$^+$ cells and, accordingly, satisfactory behavioral functional recovery. However, transplanted D16 cells were less capable of producing functional recovery. These findings provide a valuable guideline for standardizing the differentiation stage of the transplantable cells used in clinical cell therapy for PD. STEM CELLS TRANSLATIONAL MEDICINE *2017;00:000–000*

SIGNIFICANCE STATEMENT

Cell replacement is considered the promising treatment for PD. Nevertheless, no detailed and systematic study has been conducted to identify which differentiation stages of mDA cells are most suitable for transplantation in PD therapy. The present study showed that the immature mDA neurons were with the best TH$^+$ differentiation and able to recover rotation behaviour in PD mice. In contrast, mDA progenitors showed discouraging TH$^+$ differentiation and no behavioral recovery.

INTRODUCTION

Parkinson's disease (PD) is a progressive neurodegenerative disease that is characterized by the loss of dopaminergic (DA) neurons in the substantia nigra. This leads to the reduction of dopamine in the striatum, resulting in the impaired control of movements. Current pharmacological medications for PD, such as L-dihydroxyphenylalanine (L-DOPA), can only alleviate the PD symptoms, and there is no curative therapy for this disease [1]. Therefore, cell replacement therapy to restore the loss of DA neurons is considered a promising treatment for PD [2–5]. In the past, human fetal ventral mesencephalic (hFVM) cells have been transplanted into PD patients' brains, and clinical results demonstrated that hFVM cells survived and grew, reinnervated the denervated striatum, and ameliorated the behavioral deficits [6].

However, ethical and practical issues limit the clinical use of hFVM cells. Some patients also developed major side effects such as graft-induced dyskinesia due to the presence of serotonergic neurons in the hFVM [7]. Therefore, it is necessary to identify a novel source of DA neurons. With the advance of stem cell development, the generation of DA neurons from stem/progenitor cells, or converting somatic cells into DA neurons, could be that alternative cell source [8].

Differentiation of pluripotent stem (PS) cells toward DA neurons has been accomplished by initial neuronal induction either by co-culture with stromal cells or using small molecules and then regional specification. However, only a small fraction of differentiated cells became TH$^+$ DA neurons (∼20%) [9, 10]. Nevertheless, the viability of transplanted cells and the restoration of behavior

following intrastriatal transplantation of human embryonic stem cell (hESC)-derived DA neurons in a rat PD model were first reported in 2006 [11]. There were, however, considerable safety concerns regarding the risk of tumor formation or neural overgrowth. Then, in 2011, Kriks et al. [12] used a floor-plate method to generate DA neurons with midbrain identities. The viability and function of the grafted neurons were demonstrated in animal models of PD, and no tumorigenic potential was observed. Moreover, Grealish et al. [13] reported that hESC-derived DA neurons (using the floor-plate method) implanted in a rat PD model presented axonal growth and long-term survival as well as functional improvements similar to hFVM DA neurons. This shows that transplantation of hESC-derived DA neurons may become feasible for treating PD.

It is essential to determine the optimal properties of transplantable cells, characterized by various developmental stages, for grafting into PD animal models, and even more so in future PD patients. Currently, it is feasible to generate authentic midbrain DA (mDA) neurons in dishes. Different differentiation stages of DA progenitors and neurons derived from hESCs have been separately applied for cell transplantations in vivo and have been shown to survive well and restore motor deficits [12–14]. However, there is a lack of systematic study to determine which stage of differentiated cells (progenitors or neurons) produces the best long-term survival and functional restoration when grafted in vivo. Here, we performed a careful assessment of the engraftment efficacy, long-term survival, differentiation potential, maturation, and functional recovery of hESC-derived midbrain DA progenitors and DA neurons in a mouse model of PD. We selected three stages of differentiated DA cells: stage 1, mDA progenitors (day 16; characterized by high expression of FOXA2$^+$/LMX1A$^+$); stage 2, immature mDA neurons (day 25; characterized by NURR1$^+$ expression); and stage 3, mDA neurons (day 35; characterized by extended neurite outgrowth) for transplantation into a 6-hydroxydopamine (6-OHDA) induced PD mouse model.

We showed that, firstly, all three developmental stages of mDA cells can be effectively engrafted into host brains with very high viability rates, with no sign of neural overgrowth, necrosis, or apoptosis. Secondly, the ability of mDA progenitors (D16) to mature and to differentiate into TH$^+$ neurons was limited even at 3 months post-transplantation, and they therefore proved ineffective for behavioral recovery when transplanted into a 6-OHDA-induced mouse model of PD. By contrast, D25 and D35 mDA neurons showed satisfactory TH$^+$ differentiation and behavioral recovery. Finally, the transplanted mDA cells sent out widespread neurites to innervate multiple brain regions. In summary, our studies provide an effective approach for determining the developmental status of transplantable cells for future PD therapeutic applications.

MATERIALS AND METHODS

Animals

Use of the experimental animals was conducted with protocols approved by the Institutional Animal Care and Use Committee (IACUC) of the National Neuroscience Institute (Singapore). The mice were maintained in a pathogen-free facility and exposed to a 12-hour light/dark cycle with food and water. Male NOD-SCID IL2Rgc-null mice (12 weeks old) were purchased (InVivos Pte Ltd, Singapore, http://www.invivos.com.sg/) and used as recipients for the cell transplantation. Efforts were made to minimize animal suffering and the number of animals used. Three to five recipient mice were analyzed in each group.

Maintenance of hESCs and DA Neuron Differentiation

The hESC line HES-3 (46, XX) was obtained from ES Cell International. HES-3 cells were maintained and expanded in mTeSR1 (STEMCELL Technologies, CA, https://www.stemcell.com/) medium on tissue culture plates coated with Geltrex (Thermo Fisher Scientific, Singapore, https://www.thermofisher.com/sg). The cells were passaged once weekly using mechanical/manual dissociation.

The DA neuron differentiation method was derived from a floor plate (FP)-based protocol [12, 15, 16] and modified from Kirkeby et al. [15]. EBs were formed and cultured in FP medium (DMEM/F12:Neurobasal (1:1), N2 supplement (1:100), and B27 supplement without vitamin A (1:50)) in the presence of 10 μM Y-27632 (Rock inhibitor), 10 μM SB431542 (SB), 0.2 μM LDN193189 (LDN), 100 ng/ml SHH-C24II (Shh) (R&D SYSTEM, USA), 2 μM purmorphamine (pur), and 0.8 μM CHIR99021 (CHIR) for the first 4 days of differentiation. On day 4, the EBs were plated onto tissue culture plates coated with Geltrex and grown in FP medium supplemented with 0.2 μM LDN193189, 2 μM purmorphamine, and 0.8 μM CHIR99021. On day 11 of differentiation, the cell clusters were dissociated with Accutase (Thermo Fisher Scientific) and replated onto Geltrex-coated plates in droplets of 1,000,000 cells/100 μl in ND medium (Neurobasal, B27 supplement without vitamin A (1:50), brain-derived neurotrophic factor (BDNF) (10 ng/ml) (Peprotech, US, https://www.peprotech.com), glial cell line-derived neurotrophic factor (GDNF) (10 ng/ml) (Peprotech), TGF-β3 (1 ng/ml) (Peprotech) and ascorbic acid (200 mM) (Sigma-Aldrich, Singapore, https://www.sigmaaldrich.com/)). Beginning on day 13, db-cAMP (0.5 μM, Sigma-Aldrich) or DAPT (5 μM) was added to the ND medium for terminal differentiation. All small molecules were purchased from Selleckchem. The electrophysiological recording method was as described previously [17].

Generation of Cell Aggregates for Transplantation

Different stages of differentiated DA progenitors and neurons were harvested and formed into cell aggregates of uniform size (5,000 cells/aggregate) by using AggreWell 800-μM plates (STEMCELL Technologies). Cell aggregates were 200 μm in diameter 2 days before transplantation. Approximately 20 aggregates were delivered per transplantation.

Flow Cytometry

For the immunostaining of live cells, cells were dissociated into single cells and incubated with primary antibodies diluted in FACS solution (1% BSA in PBS) at 4°C for 30 minutes. Diluted fluorescent secondary antibodies were applied for conjugation of the appropriate primary antibodies, and they were incubated at 4°C for 20 minutes. Fluorescence was measured using a flow cytometer (GUAVA, Millipore, Singapore, https://www.merckmillipore.com/SG). To measure the TH/TUJ1 population of differentiated cells, cells were dissociated and fixed in 4% paraformaldehyde (PFA) at room temperature (RT) for 10 minutes. Then, they were permeabilized with 0.3% saponin (Sigma-Aldrich) in PBS and incubated with anti-TH antibody (Pel-Freez, US, http://www.pelfreez-bio.com/) at 4°C for 30 minutes with gentle shaking platform. After washing with washing buffer (0.03% saponin in PBS), the cells were incubated with Alexa Fluor 647-conjugated goat anti-rabbit IgG (H+L) and Alexa Fluor 488-conjugated mouse anti-β-tubulin

(BD Pharmingen, Singapore, https://www.bdbiosciences.com/sg/) at 4°C for 30 minutes. After being washed with washing buffer, cells were resuspended in PBS. Fluorescence was measured using a flow cytometer (GUAVA, Millipore).

Gene Expression Analysis

Total RNA was isolated with the Direct-zol RNA Purification Kit according to the manufacturer's protocol (Zymo Research, US, https://www.zymoresearch.com). The concentration and quality of purified RNA were measured using a NanoDrop device (Biofrontier Technology, Singapore, http://biofrontiertechnology.com). Then, 1 μg total RNA per sample was subjected to cDNA synthesis with the Maxima First-Strand cDNA Synthesis Kit according to the manufacturer's protocol (Thermo Scientific Fermentas). Quantitative RT-PCR was performed using TaqMan Probe-Based Gene Expression Analysis (Thermo Fisher Scientific) on a 7500 Fast Real-Time PCR System (Applied Biosystems, US, http://home.applied-biosystems.com). The TaqMan probes used in this study were listed in supplemental online Table S1. Relative mRNA expression levels of target genes were calculated based on $2^{\Delta\Delta}Ct$ formula after normalization to HPRT1 values with reference to day 0 of differentiation.

HPLC Analysis

Cultured cells were collected in 0.5N perchloric acid. The levels of dopamine (DA) and DOPAC in the differentiated cells were measured using a Reversed-phase UltiMate 3000 HPLC system (Germany) with an electrochemical detector and a reversed-phase column (DBS HYPERSIL C18, 15 cm × 3.0 mm, 3 μm, 120 Å pore size) and analyzed under the control of a Chromeleon 7.2 Chromatography Data System. The mobile phase was a mixture of 0.1 M sodium phosphate, 10 mM sodium 1-heptanesulfonate, 0.1 mM EDTA and 8% methanol (v/v), adjusted to pH 2.95 with 85% phosphoric acid. All solutions for HPLC analysis were double filtered through 0.2 μm membranes and degassed before use. The flow rate was 0.5 ml per minute. All chemicals were purchased from Sigma-Aldrich.

6-Hydroxydopamine Lesioning

Mice were anesthetized with a mixture of ketamine and diazepam (both from Ceva Animal Health PteLtd, Glenorie, Australia, http://www.ceva.com/; 100 and 20 mg/kg, respectively) and placed in a stereotaxic frame. 6-OHDA (5 μg/μl × 2 μl in 0.9% NaCl containing 0.2 mg/ml ascorbic acid) was injected into the left striatum (+0.5 mm AP, 1.8 mm ML relative to bregma and 3 mm below skull) more than 5 minutes. Two weeks later, the mice were assessed for lesion efficacy using the methamphetamine-induced rotation assay [18].

Behavioral Analysis

The methamphetamine-induced rotation assay was performed pre-transplantation and every 4 weeks after transplantation. A dose of 2.5 mg/kg of methamphetamine was injected intraperitoneally (i.p.), and the rotation behavior was recorded for 40 minutes. Animals that rotated ipsilaterally in excess of 6 turns/minute were selected for analysis [18].

Cell Transplantation

Cell transplantations were conducted one month after 6-OHDA lesion to allow SNpc DA neurons to finish cell death process, so that the transplanted cells won't affect SNpc DA neuron regeneration (supplemental online Fig. S1). The mice were anaesthetized with a mixture of ketamine and diazepamas described above and then positioned in a stereotactic injection apparatus. Suspensions of concentrated cell aggregates (1×10^5 cells in 2.5 μl) were loaded into a Hamilton microliter syringe (7105KH 5.0 μl, Hamilton Company, Bonaduz, Switzerland, https://www.hamilton-company.com/) and injected into the striatum (AP: +0.5 mm; ML: ±2 mm; DV: −3 mm). The needle was left in place for 5 minutes after the injection.

Immunocytochemistry and Immunohistochemistry (IHC) Staining

For immunocytochemistry staining, cell aggregates were fixed in 4% PFA (Sigma-Aldrich, Singapore), cryoprotected in 30% sucrose solution, cut on a cryostat and mounted on glass slides. For IHC, the mice were transcardially perfused with 4% PFA; the brains were then removed, post-fixed overnight in 4% PFA, and cryoprotected in 30% sucrose. Brain sections were cut with a cryostat and mounted on glass slides. For immunofluorescence, blocking and antibody incubations were performed with a solution of 1% BSA and 0.1% Triton X-100 (Sigma-Aldrich, Singapore) in PBS. The samples were blocked for 1 hour at RT, incubated overnight in primary antibody solutions at 4°C, and incubated for 2 hours in secondary antibody solutions at RT. After the primary and secondary antibody incubations, the sections were washed four times in PBS. The primary antibodies used were listed in supplemental online Table S2. Alexa Fluor 488/568 goat anti-rabbit/mouse IgG (1:400, Invitrogen, Singapore, https://www.thermofisher.com/us/en/home/brands/invitrogen.html) was used as secondary antibodies for fluorescence labeling. A peroxidase-conjugated goat anti-mouse secondary antibody (Vector Laboratories, Burlingame, CA, USA, https://vectorlabs.com) was used for 3,3-Diaminobenzidine (DAB) (Vector Laboratories) labeling, and positive reactions were detected by the avidin–biotin complex (ABC) method (Vector Laboratories). The slices were mounted with fluorescence mounting medium (Dako, Carpinteria, CA, USA, www.dako.com) or DPX (for IHC-DAB staining), and images were obtained with a confocal microscope (LSM710, Olympus, Tokyo, Japan, www.olympus.com).

Stereological Quantification of Grafted mDA Cells

The total numbers of grafted mDA cells that were immunoreactive for the human nucleus antigen (hNUC), Ki67, neuronal nuclei antigen (NEUN), and TH were estimated using stereological, unbiased, and systematic sampling method described before [19, 20]. Briefly, frozen coronal sections (16 μm thick) were cut and continuously collected. Stereological quantification was carried out with every 15th section to cover the entire graft from the rostral focal plane in which the grafted cells started to emerge to the caudal plane where the grafted cells disappeared. The optical images were obtained by an Olympus microscope using a 40× oil immersion objective. At least eight sections were counted for each graft. The total numbers in the grafts were calculated according to the optical fractionator equation (West, 1993, 1999).

Statistical Analysis

Statistical analyses were carried out by using GraphPad Prism Software (San Diego, CA, USA, https://www.graphpad.com/scientific-software/prism) and performed using Student's t test. All data are presented as the means and the standard deviation (mean ± SD).

Statistical significance was defined at $***p < .001$, $**p < .01$, and $*p < .05$.

In Vitro Characterization of hESC-Derived Midbrain DA Neurons Using a Floor Plate-Based Differentiation Method

To generate authentic midbrain DA (mDA) neurons, we adopted dual SMAD inhibition and FP induction protocols [12, 15, 21, 22]. The common features of these protocols are early activation of Sonic Hedgehog (Shh and Pur) and WNT (ChIR) signaling during neural induction from hESCs by dual inhibition of SMAD signaling (SB431542 and LDN) (Fig. 1A). After 16 days of neural induction, the hESC pluripotency markers TRA-1-60 (Fig. 1B) and NANOG (Fig. 1C) were undetectable. Meanwhile, the expression of the typical neural marker PSA-NCAM increased, indicating differentiation into neural progenitors (Fig. 1B). Moreover, high expression levels of FP markers (FOXA2, CORIN, and LMX1A) indicated the induction of neuronal progenitor pools with mDA characteristics on day 16 of differentiation (Fig. 1C). The co-expression of OTX2 and LMX1A revealed by immunostaining also showed that mDA progenitors were induced on day 16 (Fig. 1F). To further differentiate and mature these cells toward mDA neurons, mDA progenitors were grown in the presence of BDNF, GDNF, ascorbic acid (AA), TGF-β3, db-cAMP, and DAPT (Fig. 1A). After approximately 25 days of differentiation, the expression of NURR1 was increased, suggesting that cells at this stage acquired mDA neuronal identity, leading to the final steps toward postmitotic differentiation (Fig. 1C, 1F). From day 25 onward, TH (DA neuron marker) and MAP2 (pan-neuron marker) marked the DA neuron populations among these differentiated cells (Fig. 1D). Approximately 40% of cells were observed to be double-positive for TH and TUJ1 (Fig. 1G). By day 42 of differentiation, electrophysiological studies showed that differentiated neurons exhibited action potentials (Fig. 1H) and spontaneous postsynaptic currents (Fig. 1I). Dopamine and its metabolite DOPAC were detected in the cultures that went through further maturation at day 51 (Fig. 1J). Our results indicated that, by applying the FP-based differentiation protocol, we could obtain a high population of hESC-derived mDA neurons, and these cells presented functional neuronal properties (action potentials and synaptic transmission) and were capable of producing the neurotransmitter dopamine.

To identify the optimal stage of DA neuron differentiation for transplantation of cells for future replacement therapy in PD, we selected the three well-characterized developmental stages described above for transplantation into a mouse model of PD: stage 1, day 16 (D16) mDA progenitors, marked by high expression levels of FOXA2 and LMX1A; stage 2, day 25 (D25) immature mDA neurons, marked by NURR1 expression; and stage 3, day 35 (D35) mDA neurons, characterized by increased MAP2$^+$ expression (Fig. 1D) and extended neurite outgrowth (Fig. 1E). In addition, we modified the method of cell delivery from single cells to aggregate format. Our previous studies showed that transplanted neural aggregates exhibited a higher survival rate than single-cell preparations and that these cells were able to differentiate further into neurons and innervate host tissue (Qiu et al., 2015). Furthermore, when those cell aggregates were maintained in culture in vitro, they also presented mDA progenitor and mDA neuron identities (Fig. 1F). Therefore, cell aggregates that comprised of 5,000 cells/

aggregate were generated 2 days in advance before cell injections into the mouse model of PD.

Viability and Proliferation of the Three Developmental Stages of mDA Cells 3 Months Post-Transplantation into the Mouse Model of PD

The three developmental stages of mDA cells were transplanted as aggregates of equal cell numbers (1×10^5 cells per recipient) into NOD-SCID IL2Rgc-null mice with 6-OHDA lesions. Three months after the cell transplantation, mouse brains were perfused and sectioned. Immunohistochemistry (IHC) was performed using anti-human specific Neural cell adhesion molecule (hNCAM) and anti-human specific nucleus antigen (hNuc) antibodies to assess the survival of the transplanted mDA cells. All three types of transplants exhibited substantial viability at 3 months post-transplantation, as indicated by the IHC-DAB staining with hNCAM antibody (Fig. 2A) and the immunofluorescence (IF) staining with hNuc (Fig. 2B). Necrosis was not detected (Fig. 2A). The numbers of viable grafted cells per graft were assessed by stereologically counting the hNuc$^+$ nuclei. On average, approximately 2.4×10^5 cells survived per graft at 3 months post-transplantation found with the D16 mDA progenitors (Fig. 2C). In contrast, only approximately 1.0×10^5 and 0.7×10^5 cells per graft survived in the D25 and D35 mDA neuron transplantation, respectively (Fig. 2C), significantly fewer cells than with D16 mDA progenitor transplantation. The overall high viability rate of the transplanted cells was likely due to our preparation of the transplantable cells as cell aggregates [23–25].

To evaluate the proliferation potential of the transplanted cells, anti Ki67 antibody was used to detect any proliferating cells [26]. It was estimated that the D16 mDA progenitor transplants contained approximately 1.8% proliferating cells and that the D25 and D35 mDA neuron transplants each contained approximately 0.5% proliferating cells (Fig. 2D). The percentage of proliferating cells was not significantly different among these three types of transplantation (Fig. 2D). An apoptosis marker, cleaved caspase 3 (C-CASP3), was occasionally (1–2 cells per graft) detected in some grafts, but it was undetectable in most cases (supplemental online Fig. S2). Our results indicated that, when delivered as cell aggregates, all three cell types showed very high viability, no sign of overgrowth, and no sign of cell death.

Neuronal Differentiation and Maturation of the Three Developmental Stages of mDA Cells at 3 Months Post-Transplantation

We subsequently examined the differentiation potential of the transplanted cells and their capacity to mature in vivo. As shown in Fig. 3A, immunostaining for TUJ1 in all three types of transplants indicated the neuronal phenotype of the transplanted cells (indicated by hNCAM staining) (Fig. 3A). In contrast, only a small fraction of engrafted cells were found to be GFAP-positive astrocytes (supplemental online Fig. S3).

Moreover, we found that a significant fraction of the transplanted cells matured into NEUN-positive cells in each of the three types of transplants (Fig. 3B). Of the engrafted D25 mDA cells, 40.5% were NEUN positive, whereas the D16 and D35 transplants contained 29.7% and 28.9% NEUN-positive cells, respectively. However, the differences among the three groups were not significant (Fig. 3C). Notably, the IF intensity of the NEUN staining was much weaker in D16 mDA progenitor transplants compared to that in D25 and D35 mDA neuron transplants (Fig. 3B). These
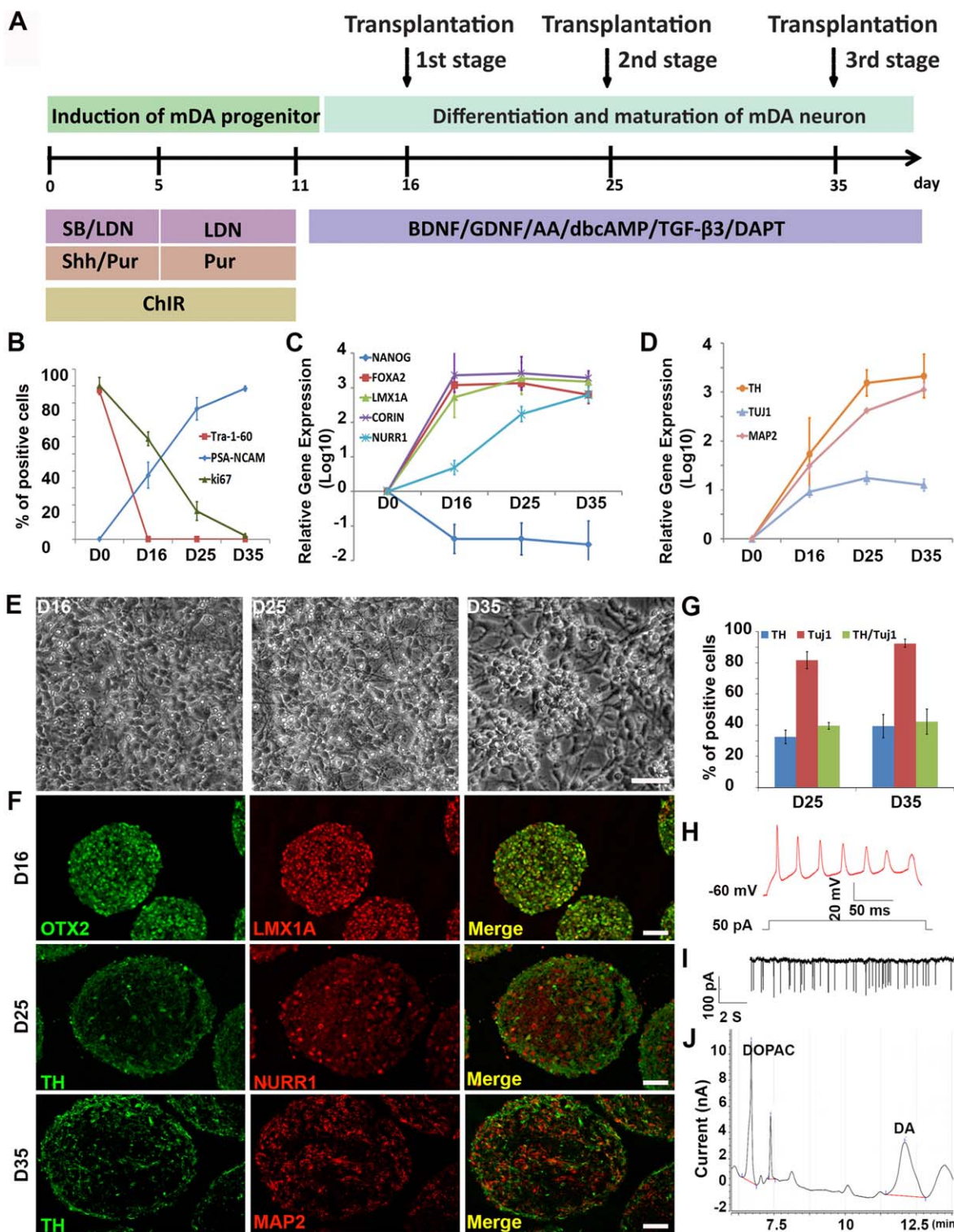
Figure 1. Differentiation and characterization of hESC-derived mDA neurons. **(A)**: An overview of the floor plate (FP)-based mDA neuron differentiation protocol and stages for transplantation. **(B)**: Flow cytometric analysis and, **(C)** and **(D)** quantitative RT-PCR analysis of gene expression levels at different stages of differentiation. Data are shown as the mean ± SD, $n = 3$ (independent experiments). **(E)**: Morphology of mDA cells at different stages of differentiation. Scale bar: 50 μm. **(F)**: Immunofluorescence images of various stages of cell aggregates on day 16 (OTX2/LMX1A), day 25 (TH/NURR1), and day 35 (TH/MAP2). Scale bar: 50 μm. **(G)**: Quantification of TH$^+$ and Tuj1$^+$ cell populations on day 25 and day 35 by flow cytometry. **(H)**: Action potential induced by 50 pA current recorded from hESC-derived neurons on day 42. **(I)**: Spontaneous postsynaptic current at Vm = −60 mV recorded from hESC-derived neurons on day 42. **(J)**: HPLC analysis of dopamine and its metabolite, DOPAC, from differentiated cells on day 51. Abbreviations: hESC, human embryonic stem cell; mDA, midbrain dopaminergic.
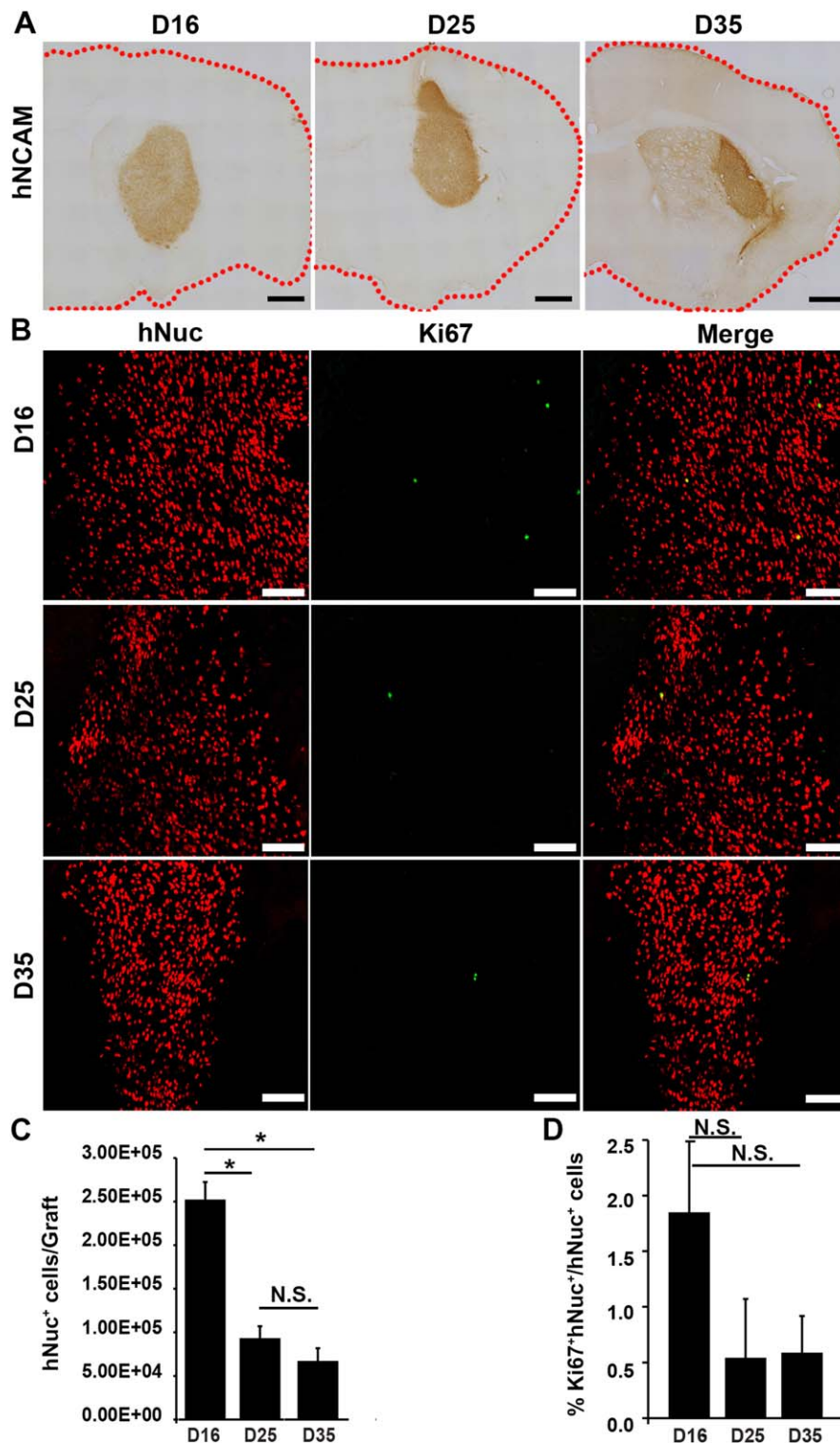
Figure 2. The survival and proliferation of the transplanted cells 3 months post-transplantation. **(A)**: IHC-DAB staining using human-specific NCAM (hNCAM) antibody show the graft sizes of transplantations of the three stages of mDA cells. Red dotted lines outline coronal sections of the right cortical hemisphere. Scale bar: 600 μm. **(B)**: Representative images showing the survival and proliferation of three stages of mDA cells. hNUC staining revealing the surviving transplanted cells. Ki67 staining showed the proliferating cells among the transplanted cells. Scale bar: 100 μm. **(C)**: Bar chart showing the quantification of the surviving transplanted cells in the three types of transplants. Data are shown as the means ± SD, $n = 3$ animals, Student's t test (two-tailed), *$p < .05$. **(D)**: Bar chart showing the percentage of proliferating cells among the grafted cells in the three types of transplants. Data are shown as the means ± SD, $n = 3$ animals, Student's t test (two-tailed). Abbreviations: IHC, Immunohistochemistry; DAB, 3,3-Diaminobenzidine; mDA, midbrain dopaminergic; hNUC, Human specific nuclear antigen.
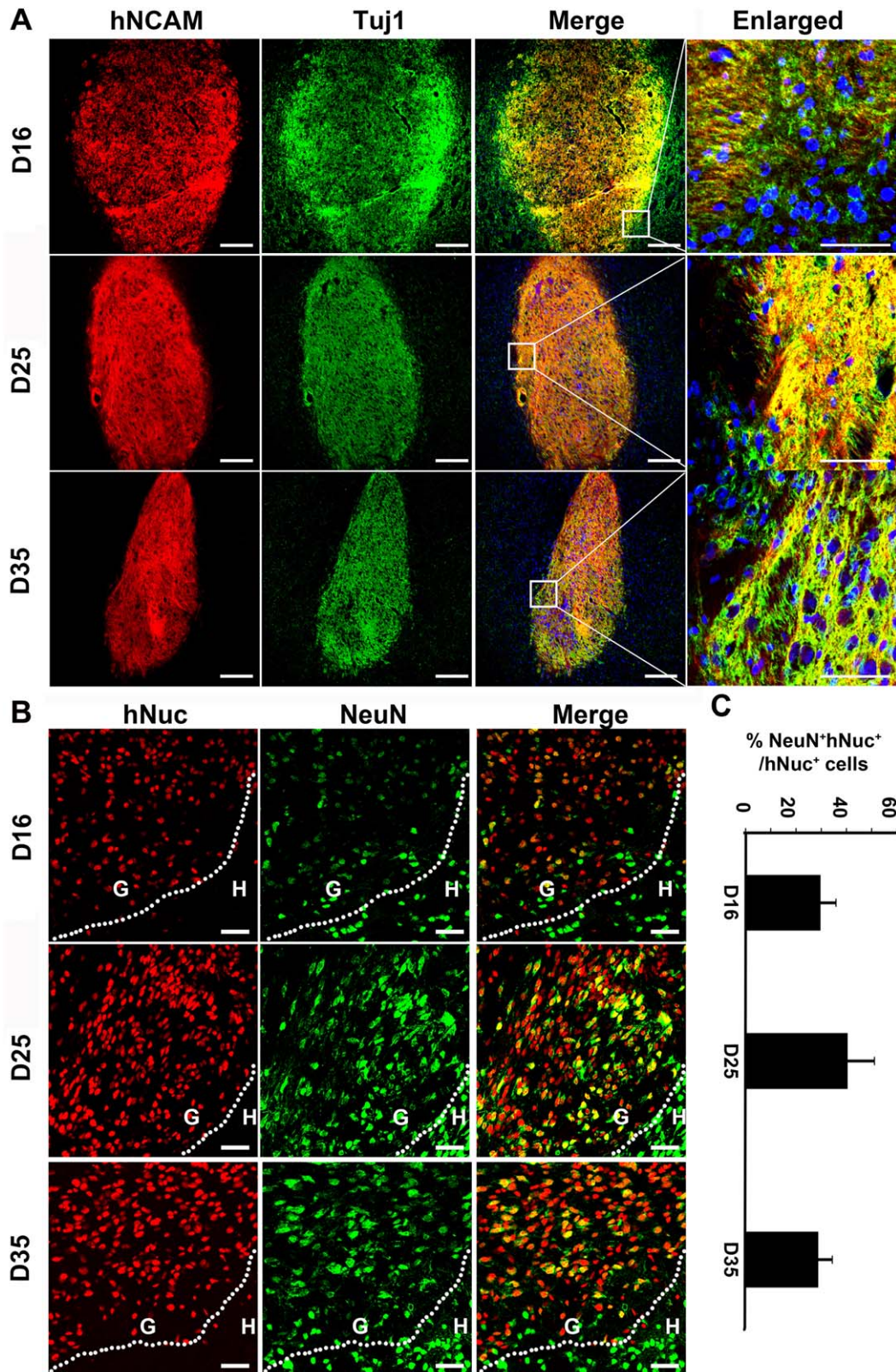
Figure 3. Neuronal differentiation and maturation of three types of transplants. **(A)**: The majority of the transplanted cells (labeled with hNCAM, red) differentiated into neurons (labeled with TUJ1, green). Scale bars: 50 μm in enlarged panel, 200 μm in other panels. **(B)**: Representative images showing the mature neurons (labeled with NEUN, green) derived from the transplanted D16, D25, and D35 mDA cells (labeled with hNUC, red) 3 months post-transplantation. G: grafted cells; H: host tissue. Scale bar: 50 μm. **(C)**: Bar chart showing the percentage of the mature neurons among the surviving transplanted cells in the three types of transplants. Data are shown as the means ± SD, $n = 3$ animals, Student's t test (two-tailed). Abbreviations: mDA, midbrain dopaminergic; hNUC, Human specific nuclear antigen.
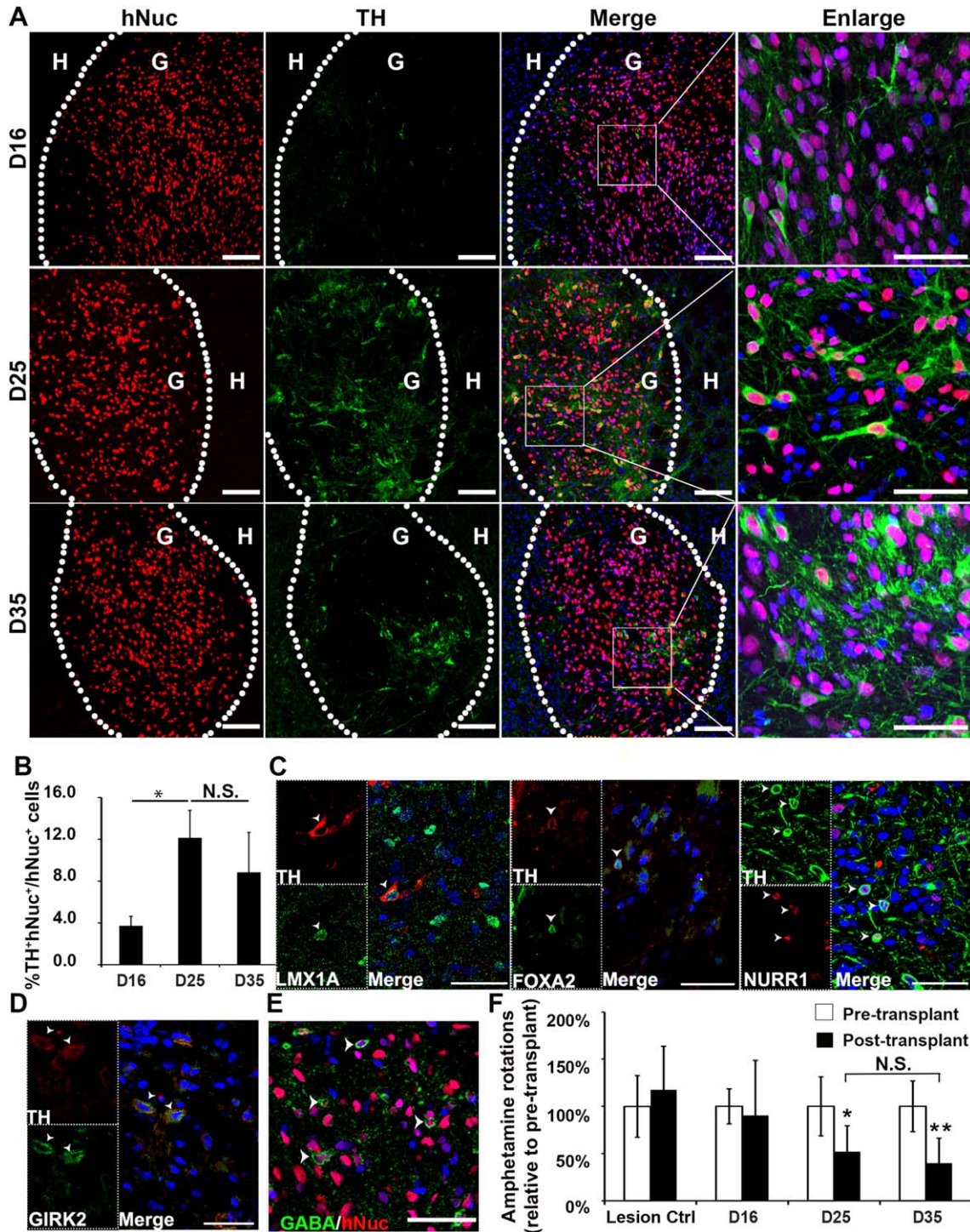
Figure 4. Comparison of the functional efficacy of the three types of transplants. **(A):** Subsets of the transplanted cells (hNUC positive, red) could differentiate into TH$^+$ DA neurons (green). G: graft region; H: host tissue. Scale bar: 50 μm in enlarged images, 100 μm in the other images. **(B):** Bar chart showing the percentage of mDA neurons among the surviving transplanted cells for the three types of transplants. Data are shown as the means ± SD, $n = 3$ animals, Student's t test (two-tailed). **(C):** Immunofluorescence images showing the co-expression of TH with midbrain neuronal markers, LMX1A, FOXA2, and NURR1, in the grafted D25 mDA neurons. 4′,6-diamidino-2-phenylindole (DAPI) (blue) indicates cell nuclei. White arrowheads indicate the cell bodies of double-positive cells. Scale bar: 50 μm. **(D):** Immunofluorescence images showing the co-expression of TH with A9 subtype marker, GIRK2, in the grafted D25 mDA neurons. DAPI (blue) indicates cell nuclei. White arrowheads indicate the cell bodies of double-positive cells. Scale bar: 50 μm. **(E):** Some of the transplanted cells (hNUC positive, red) could differentiate into GABAergic neurons (green). White arrowheads indicate GABAergic neurons. Scale bar: 50 μm. **(F):** Bar chart showing the efficacy of behavioral recovery produced by the three types of transplants. Amphetamine-induced ipsilateral rotations recorded 3 months post-transplantation were compared with rotations recorded pre-transplantation. Data are presented as percentages normalized to the pre-transplantation recordings. The values represented means ± SD, $n = 5$ animals, Student's t test (two-tailed), *$p < .05$, **$p < .01$. Abbreviations: mDA, midbrain dopaminergic; hNUC, Human specific nuclear antigen.

results indicated that although all three developmental stages of mDA cells were able to differentiate into neurons, D25 immature mDA neuron transplants showed the highest proportion of mature neurons when compared to the other two groups.

Functional Efficiency of the Three Developmental Stages of mDA Neurons in PD Mouse

We next proceeded to assess the functional efficacy of these three developmental stages of mDA cells 3 months post-transplantation. TH$^+$ neurons were found in all grafts of the three mDA cell types. The grafted TH$^+$ neurons were located in both the center and periphery of the transplant regions (Fig. 4A). Among the three transplantation groups, D25 mDA neuron transplants showed the highest percentage of TH$^+$ neurons among the total grafted cells (12.14%). This percentage was significantly higher than D16 mDA progenitor transplants (3.73%) and was also somewhat but not significantly higher than that in D35 mDA neuron transplants (8.85%) (Fig. 4B). For both D16 and D25 cells, the TH$^+$ cells were evenly distributed within the graft, whereas the TH$^+$ cells in D35 transplants tended to be more concentrated in sub-regions of the grafts (Fig. 4A). The grafted TH$^+$ cells also reliably expressed midbrain neuronal marker, LMX1A, FOXA2 and, NURR1 (Fig. 4C), and A9 DA subtype marker, GIRK2 (Fig. 4D), indicating they were the functional components in the grafts. Notably, in all three types of transplants, GABAergic neurons were detected in subsets of the grafted cells (Fig. 4E). In contrast, we did not observe serotonergic neurons in any of the three types of transplants (supplemental online Fig. S4). Together, these results demonstrated that all three types of mDA cells were capable to differentiate into mDA neurons with D25 mDA cells achieved the most efficient TH$^+$ mDA neuronal in vivo differentiation efficiency.

In addition, we evaluated the ability of these three types of transplants to rescue the amphetamine-induced rotation behavior in Parkinsonian mice. Both the D25 and D35 mDA neuron transplants were able to significantly reduce the abnormal rotations at 3 months post-transplantation (Fig. 4F). No significant difference was observed between D25 and D35 transplants in the rescue efficacy (50% reduction versus 60% reduction respectively). In contrast, the D16 mDA progenitor transplants did not show significant behavioral improvement by 3 months post-transplantation (Fig. 4F). This was consistent with the above finding that D16 mDA progenitors showed weaker neuronal maturation and TH$^+$ neuron differentiation compared to D25 and D35 transplants.

Integration of the Transplanted Cells into the Host Tissues

One important criterion for evaluating whether transplanted cells are suitable for clinical therapy is to assess the integration of these cells into the host tissue [27, 28]. Given that the D25 mDA neurons showed the best TH$^+$ differentiation (Fig. 4B) and able to recover rotation behaviour in PD mice (Fig. 4F), to assess the integration of the transplanted D25 mDA neurons, we examined the neurite targeting and migration of the engrafted cells. Three months post-transplantation, the transplanted cells exhibited extensive fiber outgrowth and innervated multiple regions of the host brain. The neurite outgrowth pattern was examined in both sagittal (Fig. 5A–5C) and coronal (Fig. 5D–5H) brain sections, as shown by the dense hNCAM staining of the neurites of the transplanted cells. To target nearby areas, engrafted cells innervated the ipsilateral striatum (Fig. 5B, 5H) and both the ipsilateral and contralateral septum (Fig. 5E). To target remote areas, engrafted

cells sent out fibers along white matter tracts, including the corpus callosum to innervate the ipsilateral and contralateral piriform cortex (Fig. 5F, 5G) and the cerebral peduncle (Fig. 5C).

In contrast to the widespread neurite innervation, the migration of the transplanted cells was limited, with only approximately 100 μm of migration out from the transplanted core within the striatum (the regions between the pairs of dotted lines in Fig. 5I). Notably, there were numerous cells from the host brain present within the transplant region (Fig. 5I), suggesting an efficient integration between the transplanted cells and the host tissue.

DISCUSSION

The transplantation of DA neurons is considered as a potential therapeutic cell based treatment for PD, and the DA neurons derived from human PS cells (hPSCs) have attracted significant interest. Prior to transplantation, three fundamental aspects must be addressed: the identification of a transplantable stage during DA neuron differentiation, in vivo DA neuronal survival, and functional assessment [10]. Currently, efficient DA neuron generation has been produced using FP-based methods [8, 12, 13, 15, 21, 29–31]. Different stages of DA cells have been examined individually in vivo and different conclusions have been reached [12–16]. This study for the first time used three differentiated stages of cells generated by a FP-based protocol: DA progenitors (D16), post-mitotic immature DA neurons (D25) and DA neurons (D35), and systematically examined the competence of these cells in cell-transplantation therapy in a mouse model of PD.

The clinical studies have indicated that midbrain DA progenitors, which appear post conception week 6–9 in human [29, 31, 32], are the most therapeutically effective when transplanted to cure PD [33]. Based on the expression curve of FOXA2 and CORIN, the D16 mDA cells generated in this study using the FP-based differentiation protocol are equivalent to this stage (Fig. 1B, 1C). These progenitors were preferred in clinic because of their high survivability compared to the more differentiated cells. This was consistent to our finding that the number of engrafted cells from D16 DA progenitors was significantly higher than those from the other two groups 3 months post-transplantation (Fig. 2C). However, the DA linage differentiation and maturation were poorer for the D16 DA progenitors and resulted in poor functional rescue of the amphetamine-induced rotation behavior (Fig. 4). Although D16 DA progenitors have been shown to be effective to rescue behavioral impairment in PD mouse in previous studies [13, 15], more recent and comprehensive study from the same research group admitted that D16 DA progenitors are not effective to rescue the behavioral impairment even at 16 weeks post transplantation [34]. The effect of the D16 transplants can only be seen at 22–25 weeks post transplantation [34]. It is possible that the percentage of TH-positive cells among the D16 mDA progenitors might increase and acquire functionality over a longer period of time, which would be outside the time window described in this study (12 weeks post transplantation). Moreover, the percentage of TH$^+$ cells among total transplanted cells was reported to be around 3.7% in D16 transplants [34], which is consistent with our current finding (Fig. 4) and much lower than the DA yield of the D25 transplants (Fig. 4). Together, these findings undermined the utilization value of the D16 DA progenitors.

As mentioned above, one concern for transplanting more differentiated DA cells is their poor survivability in vivo. Strikingly, by
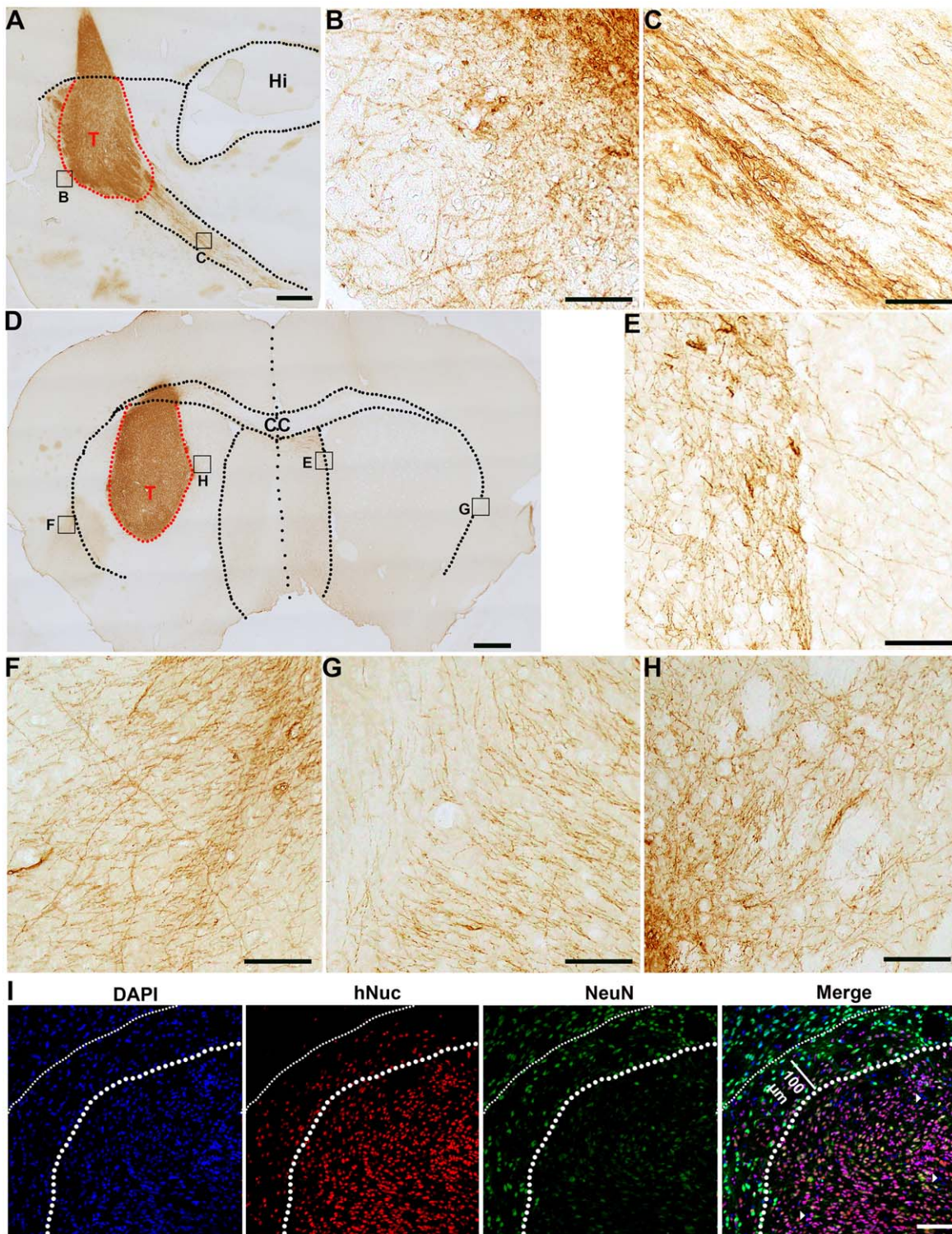
Figure 5. The transplanted D25 mDA neurons innervated multiple brain regions. IHC-DAB staining using hNCAM antibody revealed the projections of the transplanted human ES-derived D25 mDA neurons. **(A)**: Sagittal section showed that the transplanted cells residing in the transplanted core (T) innervated the surrounding striatum **(B)** and projected toward the pons and cerebellum through the cerebral peduncle **(C)**. **(D)**: Coronal section showed that the transplanted cells residing in the transplanted core innervated the septal nuclei **(E)**, the ipsilateral-piriform cortex **(F)**, the contralateral piriform cortex **(G)**, and the surrounding striatum **(H)**. **(I)**: The migration of transplanted cells from the transplantation core to the surrounding striatum. The thick dotted line outlined the edge of the transplantation core region. The thin dotted line indicates the frontier of the migrated transplanted cells. White arrows indicate host cells present in the transplantation core region. T: transplanted core; Hi: hippocampus; CC: corpus callosum. Scale bars: 500 μm in **(A)** and **(D)**; 50 μm in **(B)**, **(C)**, **(E–H)**; 100 μm in **(I)**. Abbreviations: IHC, immunohistochemistry; DAB, 3,3-diaminobenzidine; mDA, midbrain dopaminergic.

forming aggregates of post-mitotic DA neurons and transplanting those aggregates 2 days later, we managed to achieve more than 70% survival rate in D25 and D35 mDA neuronal transplants (Fig. 2C). This modification of cell delivery [24] enabled the utilization of more safer and authentically differentiated DA neurons, since there is only around 0.5% proliferating cells in D25 and D35 DA neuronal transplants (Fig. 2D). Both D25 and D35 mDA transplants resulted in functional rescued behavior in Parkinsonian mice in this study. However, considering that even a small number of surviving TH$^+$ cells can significantly rescue amphetamine induced asymmetric rotation in PD mouse, histology analysis is more reliable to evaluate the therapeutic efficacy of the transplanted cells. Our results showed that the D35 transplants produced fewer engrafted mature NEUN$^+$ and TH$^+$ cells than the D25 transplants. This is consistent with previous report (Doi et al., 2014) and probably due to the inherent poor survivability of mature neurons with extensive neuritis, as has been reported [12]. Thus, current findings synergistically indicated D25 post-mitotic immature mDA neurons to be a favorable differentiation stage for transplantation in terms of their survival ability, maturation, and mDA neuron differentiation.

Notably, the neurites sent out from transplanted cells innervate not only the surrounding striatum but also other brain areas. This is consistent with reported observations [35]. In this study, dense hNCAM-stained neuronal fibers can be found in the septal nuclei and piriform cortex. Both of these two regions receive significant DA input from the midbrain and are important structures involved in the reward pathway [36]. The heterogeneity of the engrafted neurons might be the cause of the innervation of multiple regions in the brain. It will be of interest to investigate whether transplanting mDA neurons of higher purity can alleviate the multiple region innervations.

Conclusion

In conclusion, our study shows the importance of identifying the most suitable cells at an appropriate differentiation stage for achieving safe and efficacious DA neuron engraftment. We identified post-mitotic immature DA neurons (D25, high NURR1 expression) as the most suitable cell source for future PD cell therapy. Cell types at earlier or later stages of differentiation were not suitable due to their immaturity and reduced in vivo survivability, respectively. For future therapeutic application, we believe that further research is needed to characterize the post-mitotic immature DA neurons and to develop a more scalable production method tailored for this population to ensure the consistency, efficacy, and safety of the therapy.

Author Contributions

L.Q. and M.C.L.: conception and design; acquisition of data; draft the article; A.K.C., Z.Z., S.W., S. X., and S.R.: acquisition of data; W.H. supervise experiments and edit manuscript; E.K.T., S.K.W.O., and L.Z.: conception and design; analysis and interpretation of data; supervise all experiments; edit the article. All authors read and approved the manuscirpt.

Disclosure of Potential Conflicts of Interest

E.K.T.: Honoraria as an editor for European Journal of Neurology and Parkinsonism & Related Disorders Research funding from the National Medical Research Council. The other authors indicated no potential conflicts of interest.

References

1 Nishimura K, Takahashi J. Therapeutic application of stem cell technology toward the treatment of Parkinson's disease. Biol Pharm Bull 2013;36:171–175.

2 Bega D, Krainc D. Long-term clinical outcomes after fetal cell transplantation in Parkinson disease: Implications for the future of cell therapy. JAMA 2014;311:617–618.

3 Lindvall O, Brundin P, Widner H et al. Grafts of fetal dopamine neurons survive and improve motor function in Parkinson's disease. Science 1990;247:574–577.

4 Hallett PJ, Cooper O, Sadi D et al. Long-term health of dopaminergic neuron transplants in Parkinson's disease patients. Cell Rep 2014;7:1755–1761.

5 Kefalopoulou Z, Politis M, Piccini P et al. Long-term clinical outcome of fetal cell transplantation for Parkinson disease: Two case reports. JAMA Neurol 2014;71:83–87.

6 Barker RA, Barrett J, Mason SL et al. Fetal dopaminergic transplantation trials and the future of neural grafting in Parkinson's disease. Lancet Neurol 2013;12:84–91.

7 Barker RA, Kuan WL. Graft-induced dyskinesias in Parkinson's disease: What is it all about? Cell Stem Cell 2010;7:148–149.

8 Zhu B, Caldwell M, Song B. Development of stem cell-based therapies for Parkinson's disease. Int J Neurosci 2016;126:955–962.

9 Cho MS, Lee YE, Kim JY et al. Highly efficient and large-scale generation of functional dopamine neurons from human embryonic stem cells. Proc Natl Acad Sci USA 2008;105: 3392–3397.

10 Ganat YM, Calder EL, Kriks S et al. Identification of embryonic stem cell-derived midbrain dopaminergic neurons for engraftment. J Clin Invest 2012;122:2928–2939.

11 Roy NS, Cleren C, Singh SK et al. Functional engraftment of human ES cell-derived dopaminergic neurons enriched by coculture with telomerase-immortalized midbrain astrocytes. Nat Med 2006;12:1259–1268.

12 Kriks S, Shim JW, Piao J et al. Dopamine neurons derived from human ES cells efficiently engraft in animal models of Parkinson's disease. Nature 2011;480:547–551.

13 Grealish S, Diguet E, Kirkeby A et al. Human ESC-derived dopamine neurons show similar preclinical efficacy and potency to fetal neurons when grafted in a rat model of Parkinson's disease. Cell Stem Cell 2014;15:653–665.

14 Doi D, Samata B, Katsukawa M et al. Isolation of human induced pluripotent stem cell-derived dopaminergic progenitors by cell sorting for successful transplantation. Stem Cell Reports 2014;2:337–350.

15 Kirkeby A, Grealish S, Wolf DA et al. Generation of regionally specified neural progenitors and functional neurons from human embryonic stem cells under defined conditions. Cell Rep 2012;1:703–714.

16 Xi J, Liu Y, Liu H et al. Specification of midbrain dopamine neurons from primate pluripotent stem cells. Stem Cells 2012;30: 1655–1663.

17 Wu SM, Tan KS, Chen H et al. Enhanced production of neuroprogenitors, dopaminergic neurons, and identification of target genes by overexpression of sonic hedgehog in human embryonic stem cells. Stem Cells Dev 2012;21: 729–741.

18 Nikkhah G, Olsson M, Eberhard J et al. A microtransplantation approach for cell suspension grafting in the rat Parkinson model: A

detailed account of the methodology. Neuroscience 1994;63:57–72.

19 West MJ. New stereological methods for counting neurons. Neurobiol Aging 1993; 14:275–285.

20 West MJ. Stereological methods for estimating the total number of neurons and synapses: issues of precision and bias. Trends Neurosci 1999;22:51–61.

21 Chambers SM, Fasano CA, Papapetrou EP et al. Highly efficient neural conversion of human ES and iPS cells by dual inhibition of SMAD signaling. Nat Biotechnol 2009;27:275–280.

22 Gonzalez R, Garitaonandia I, Abramihina T et al. Deriving dopaminergic neurons for clinical use. A practical approach. Sci Rep 2013;3:1463.

23 Frisch SM, Francis H. Disruption of epithelial cell-matrix interactions induces apoptosis. J Cell Biol 1994;124:619–626.

24 Qiu L, Lim YM, Chen AK et al. Microcarrier-expanded neural progenitor cells can survive, differentiate, and innervate host neurons better when transplanted as aggregates. Cell Transplant 2015;25:1343–1357.

25 Soto-Gutierrez A, Yagi H, Uygun BE et al. Cell delivery: From cell transplantation to organ engineering. Cell Transplant 2010;19: 655–665.

26 Zhang W, Zhang W, Thevapriya S et al. Amyloid precursor protein regulates neurogenesis by antagonizing miR-574–5p in the developing cerebral cortex. Nat Commun 2014;5:3330.

27 Grealish S, Jönsson ME, Li M et al., The A9 dopamine neuron component in grafts of ventral mesencephalon is an important determinant for recovery of motor function in a rat model of Parkinson's disease. Brain 2010; 133(Pt 2):482–495.

28 Mendez I, Sanchez-Pernaute R, Cooper O et al., Cell type analysis of functional fetal dopamine cell suspension transplants in the striatum and substantia nigra of patients with Parkinson's disease. Brain 2005;128(Pt 7): 1498–1510.

29 Gale E, Li M. Midbrain dopaminergic neuron fate specification: Of mice and embryonic stem cells. Mol Brain 2008;1:8.

30 Steiner D, Khaner H, Cohen M et al. Derivation, propagation and controlled differentiation of human embryonic stem cells in suspension. Nat Biotechnol 2010;28:361–364.

31 Smidt MP, Burbach JP. How to make a mesodiencephalic dopaminergic neuron. Nat Rev Neurosci 2007;8:21–32.

32 Peng SP, Copray S. Comparison of human primary with human iPS cell-derived dopaminergic neuron grafts in the rat model for Parkinson's disease. Stem Cell Rev 2016; 12:105–120.

33 Singec I, Jandial R, Crain A et al. The leading edge of stem cell therapeutics. Annu Rev Med 2007;58:313–328.

34 Kirkeby A, Nolbrant S, Tiklova K et al. Predictive markers guide differentiation to improve graft outcome in clinical translation of hESC-based therapy for Parkinson's disease. Cell Stem Cell 2017;20:135–148.

35 Thompson L, Barraud P, Andersson E et al. Identification of dopaminergic neurons of nigral and ventral tegmental area subtypes in grafts of fetal ventral mesencephalon based on cell morphology, protein expression, and efferent projections. J Neurosci 2005;25:6467–6477.

36 Hargus G, Cooper O, Deleidi M et al. Differentiated Parkinson patient-derived induced pluripotent stem cells grow in the adult rodent brain and reduce motor asymmetry in Parkinsonian rats. Proc Natl Acad Sci USA 2010;107:15921–15926.

See www.StemCellsTM.com for supporting information available online.